

1 Isolation of a putative S-layer protein from anammox biofilm  
2 extracellular matrix using ionic liquid extraction

3 Lan Li Wong<sup>1</sup>, Gayathri Natarajan<sup>1</sup>, Marissa Boleij<sup>2</sup>, Sara Swi Thi<sup>1</sup>, Fernaldo Richtia  
4 Winnerdy<sup>4</sup>, Sudarsan Mugunthan<sup>1</sup>, Yang Lu<sup>1</sup>, Jong-Min Lee<sup>5</sup>, Yuemei Lin<sup>2</sup>, Mark van  
5 Loosdrecht<sup>2</sup>, Yingyu Law<sup>1</sup>, Staffan Kjelleberg<sup>1,6,7</sup>, Thomas Seviour<sup>1,\*</sup>.

6  
7 **Affiliations:**

8 <sup>1</sup> Singapore Centre for Environmental Life Sciences Engineering, Nanyang Technological  
9 University, 637551, Singapore

10 <sup>2</sup> Department of Biotechnology, Delft University of Technology, 2629 HZ, Delft, The  
11 Netherlands.

12 <sup>3</sup> School of Physical and Mathematical Sciences, Nanyang Technological University, 637371,  
13 Singapore.

14 <sup>4</sup> School of Chemical and Biomedical Engineering, Nanyang Technological University, 62  
15 Nanyang Drive, 637459, Singapore

16 <sup>5</sup> School of Biological Sciences, Nanyang Technological University, 637551, Singapore.

17 <sup>6</sup> Centre for Marine Bio-Innovation, School of Biological, Earth and Environmental Sciences,  
18 University of New South Wales, Sydney, 2052, Australia.

19  
20 Corresponding author: [twseviour@ntu.edu.sg](mailto:twseviour@ntu.edu.sg)  
21  
22  
23  
24

## 25 **Abstract**

26 Anaerobic ammonium oxidation (anammox) performing bacteria self-assemble into compact  
27 biofilms by expressing extracellular polymeric substances (EPS). Anammox EPS are poorly  
28 characterized, largely due to their low solubility in typical aqueous solvents. Pronase digestion  
29 achieved  $19.5 \pm 0.9$  and  $41.4 \pm 1.4\%$  (w/w) more solubilization of *Candidatus Brocadia sinica*-  
30 enriched anammox granules than DNase and amylase respectively. Nuclear magnetic resonance  
31 profiling of the granules confirmed that proteins were dominant. We applied ionic liquid (IL)  
32 1-ethyl-3-methylimidazolium acetate and N,N- dimethylacetamide (EMIM-Ac/DMAc)  
33 mixture to extract the major structural proteins. Further treatment by anion exchange  
34 chromatography isolated homologous S/T-rich proteins BROSI\_A1236 and UZ01\_01563,  
35 which were major components of the extracted proteins and sequentially highly similar to  
36 putative anammox surface-layer (S-layer) protein KUSTD1514. EMIM-Ac/DMAc extraction  
37 enriched for these putative S-layer proteins against all other major proteins, along with six  
38 monosaccharides (i.e. arabinose, xylose, rhamnose, fucose, galactose and mannose). The  
39 sugars, however, contributed  $<0.5\%$  (w/w) of total granular biomass, and were likely co-  
40 enriched as glycoprotein appendages. This study demonstrates that S-layer proteins are major  
41 constituents of anammox biofilms and can be isolated from the matrix using an ionic liquid-  
42 based solvent.

43

## 44 **Introduction**

45 Anaerobic ammonium oxidation (anammox), whereby ammonium is anaerobically oxidized  
46 directly to nitrogen gas with nitrite as electron acceptor, contributes up to 80% of oceanic N  
47 losses<sup>1</sup>, and when coupled with partial nitrification is a more sustainable option for N removal  
48 from waste waters than conventional processes<sup>2</sup>. Anammox has been researched intensively

49 over several decades across different natural environments as well as more than 100 full-scale  
50 wastewater treatment plants<sup>3</sup>. Nineteen anammox species have been identified so far with all  
51 belonging to the *Planctomycetes* phylum<sup>4</sup>. Each species, regardless of habitat, self-assembles  
52 through extracellular polymeric substances (EPS) expression, into either supported biofilms or  
53 granules<sup>5</sup>. Biofilm existence allows anammox bacteria to form syntrophic relationships with  
54 other bacteria (e.g. ammonium oxidizing bacteria)<sup>6</sup> and enhances sludge retention. EPS can also  
55 increase microbial tolerances to a range of environmental stresses, such as shear, oxidative and  
56 salinity stress<sup>7</sup>.

57 EPS have key roles in anammox biofilms. Little is known about the structure and function of  
58 specific EPS in water and wastewater biofilms<sup>8</sup>. Research into anammox EPS has largely  
59 focused on general classes of molecules<sup>9</sup>, for example changes in total protein or sugar content  
60 in response to environmental conditions like shear<sup>10</sup> and salinity stress<sup>11, 12</sup>. *In situ*  
61 characterizations have revealed the spatial distribution of proteins, polysaccharides and cells in  
62 anammox sludges. For example, loose protein secondary structure in anammox EPS has been  
63 shown to expose large amounts of hydrophobic amino acid groups for hydrophobic interactions  
64 that effectively mediate anammox EPS aggregation<sup>13</sup>. Similarly, a  $\beta$ -sheet structure of  
65 extracellular proteins in anammox granules was found to maintain the function of inner  
66 hydrophobic groups, while uronic acids further support the biofilm matrix and prevent cell  
67 detachment<sup>14</sup>. Nonetheless, the precise identities and compositions of anammox EPS remain  
68 undescribed.

69 Identifying key biopolymers within anammox EPS has always been a major challenge due to  
70 their poor solubility in conventional, typically aqueous, extraction solvents. In addition, a  
71 variety of anammox biofilm morphologies, including homogeneously-distributed<sup>15, 16</sup>, stratified  
72 granules<sup>17-20</sup>, flocs<sup>21</sup> and surface-attached<sup>22</sup> structures further confound the extraction and  
73 characterization of anammox EPS. Numerous attempts to extract anammox EPS through either

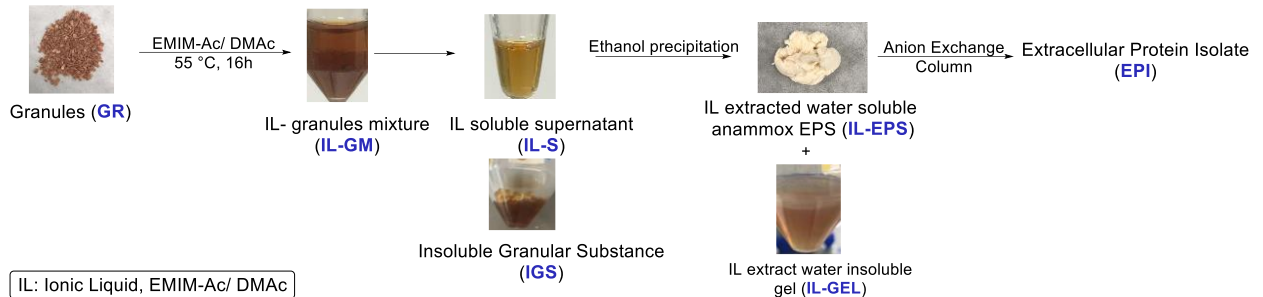
74 cationic exchange resin (CER)<sup>23</sup>, physical methods such as centrifugation, heating and  
75 sonication or chemical methods by using organic solvents (detergents and ethanol), have been  
76 made. However, to date no exopolymer has been isolated from the matrix of anammox biofilms,  
77 which is a minimum requirement for subsequent biophysical and functional analysis.

78 While some metabolic proteins are conserved between anammox species (e.g. the c-type heme  
79 proteins)<sup>24</sup>, it is unknown whether any extracellular proteins are similarly conserved. It has been  
80 reported that surface layer (S-layer) proteins may be common to anammox biofilms as a  
81 structural component of the cell. For example, KUSTD1514 forms a shell on the outside of the  
82 cell envelope of *Ca. Kuenenia stuttgartiensis*<sup>25</sup>, while a homologous S-layer protein is a major  
83 EPS constituent of *Ca. Brocadia*-enriched granular biofilm and hypothesized to also contribute  
84 to biofilm matrix structure (i.e. following shedding)<sup>26</sup>. S-layer proteins could be important to  
85 biofilm formation more broadly<sup>27</sup>. Describing a function for S-layer proteins in biofilm  
86 formation is confounded by the fact that they are embedded in EPS and the S-layer protein has  
87 not been isolated from the anammox biofilm matrix.

88 To address the challenge of processing anammox EPS, we used ionic liquid 1-ethyl-3-methyl  
89 imidazolium acetate (EMIM-Ac) to dissolve a laboratory anammox granular biofilm.  
90 Imidazolium-based ionic liquids are green solvents that have also been applied to process  
91 similarly recalcitrant biopolymers (e.g. cellulose and chitosan)<sup>28</sup>, as protein stabilizers and co-  
92 solvents, and enzyme catalysts. We extracted and purified the putative S-layer protein from a  
93 laboratory anammox granular biofilm. We found a putative S-layer protein to be the dominant  
94 polymer in our biofilm extract. While six monosaccharides were co-enriched with the EPS, they  
95 contributed <0.5% (w/w) of total granular biomass and were all common protein o-  
96 glycosylating sugars. It is thus likely that they were enriched as glycoprotein appendages rather  
97 than free exopolysaccharides. We provide further support for an important role for S-layer  
98 proteins in anammox biofilms, and present a method, involving EMIM-Ac, that allows for S-

99 layer proteins to be isolated from complex matrices such as biofilm EPS. This will inform on  
100 the role of S-layer proteins in anammox biofilm formation.

## 101 **Materials and methods**



102

103 **Figure 1: Schematic diagram of anammox extracellular polymeric substances (EPS) extraction and**  
104 **purification with ionic liquid (IL)**

105

### 106 **Anammox granular sludge enrichment**

107 Anammox granular sludges (GR) were cultivated in a 4 L reactor seeded with activated sludge  
108 from a full-scale water reclamation plant (WRP) in Singapore and fed a synthetic medium  
109 consisting of (g/L): KHCO<sub>3</sub> 1.25, KH<sub>2</sub>PO<sub>4</sub> 0.025, CaCl<sub>2</sub>·6H<sub>2</sub>O 0.3, MgSO<sub>4</sub>·7H<sub>2</sub>O 0.2 and  
110 FeSO<sub>4</sub>·7H<sub>2</sub>O 0.025. More details on laboratory anammox granules enrichment are provided in  
111 the Supporting Information (SI).

112 Granules were extracted from the reactor immediately prior to the settle and decant phase,  
113 washed with double-distilled water and lyophilized (FreeZone Plus 4.5 Liter Cascade Benchtop  
114 Freeze Dry System).

115

### 116 **Enzymatic treatment of granules**

117 Granules (GR) were digested by Pronase E, DNase A, and  $\alpha$  and  $\beta$  amylase (Sigma Aldrich,  
118 Singapore), either independently or in sequence. 2 mg/mL of each enzyme was applied to 10  
119 mg/mL biofilm in 2 mL Eppendorf tubes. An incubation time of 2 h was applied for all the  
120 treatments at 37°C (for Pronase E and DNase A) and 60°C (for  $\alpha$  and  $\beta$  amylase). Pronase E

121 (0.16% (w/w)) was prepared in 0.1 M Tris, 0.5% SDS, pH 7.5, DNase A (1% (w/w)) was  
122 prepared in 0.1 M Tris, 25 mM MgCl<sub>2</sub>, 5 mM CaCl<sub>2</sub>, pH 8.0 while  $\alpha$  and  $\beta$  amylase (25  $\mu$ L/mL  
123 and 2.5  $\mu$ L/mL) were prepared in 16 mM sodium acetate buffer, pH 6. After digestion, the  
124 supernatant was removed and the residual solids washed three times with double distilled water.  
125 Total suspended solids (TSS) and volatile suspended solids (VSS) were measured according to  
126 the APHA standard method<sup>29</sup>. TSS and VSS solubilization percentages were calculated as the  
127 percentage difference in TSS and VSS respectively before and after enzymatic treatment.

128

### 129 **EPS extraction by ionic liquid**

130 The method for extracellular polymeric substances (EPS) extraction and processing is  
131 summarized in Figure 1.

132 Freeze-dried (FreeZone Plus 4.5 Liter Cascade Benchtop Freeze Dry System) laboratory  
133 anammox granules (GR) were directly added to 40:60 (v/v) 1-ethyl-3-methyl imidazolium  
134 acetate (EMIM-Ac)/N,N-dimethylacetamide (DMAc) mixture as described by Seviour et al.<sup>30</sup>,  
135 to a concentration of 30 mg dry sludge/mL. The tube was incubated in a water bath at 55°C for  
136 16 h. The ionic liquid-soluble fraction (IL-S) was captured by precipitation with ethanol (70%  
137 (v/v)), separated by centrifugation, cleaned by dialysis and lyophilized to give IL-extracted  
138 anammox EPS (IL-EPS) for further analysis.

139

### 140 **Nuclear magnetic resonance (NMR) spectroscopy of acid-digested granules**

141 The IL-EPS fraction (37.5 mg/mL) was dissolved in 4 M trifluoroacetic acid-d (TFA-d) and  
142 heated to 120°C for 5 h. 1D <sup>1</sup>H and 2D <sup>1</sup>H-<sup>13</sup>C HSQC NMR spectra of acid-digested IL-EPS  
143 were then collected on a 700 MHz Bruker Avance II spectrometer at 25°C. Due to the high  
144 concentration of IL-EPS precipitate in the 4 M TFA-d, the required pulse length for the 90°

145 excitation pulse was extremely long. Spectra analyses were performed using Topspin 4.0  
146 (Bruker) software.

147

### 148 **<sup>31</sup>P NMR analysis of soluble EPS**

149 <sup>31</sup>P NMR solution state NMR experiments were performed on a 400 MHz Bruker Avance  
150 spectrometer at 25°C. Asolectin (30 mg/mL) (Sigma Aldrich) and anammox granules (30  
151 mg/mL) for NMR analysis were prepared in 40:60 (v/v) EMIM-Ac/DMAc. *Pseudomonas*  
152 *aeruginosa* planktonic cell lysate (30 mg/mL) was prepared by lysing the cells in lysozyme.  
153 10% (v/v) of D<sub>2</sub>O and 7.5 mM of H<sub>3</sub>PO<sub>4</sub> was added to all samples prior to NMR analysis for  
154 locking and referencing purposes. All spectral analyses were performed using Topspin 4.0  
155 (Bruker) software.

156 Briefly, overnight PAO1 WT planktonic cell pellet was resuspended in 2.25 mL of STET buffer  
157 (10 mM Tris-HCl, pH 8 with 0.1 M NaCl, 1 mM EDTA, and 5% (w/v) TRITON<sup>®</sup> X-100)  
158 followed by the addition of 258 µL, 10 mg/mL lysozyme (Sigma-Aldrich) in lysozyme solution  
159 (10 mM Tris-HCl, pH 8). The mixture was vortexed and incubated in 37°C for 3 hours followed  
160 by probe sonication (SM Vibracell CVX750 Probe Ultrasonicator) at 3s interval for 12 min.  
161 The lysate pellet was then freeze dried for NMR analysis.

162

### 163 **Staining and microscopy**

164 Microscopic imaging was conducted on a confocal microscope Leica SP8WLL and Zeiss LSM  
165 780 with a 63× objective. Briefly, crude and IL-treated anammox granules were stained with  
166 BacLight Live/Dead viability stain (Thermo Fisher Scientific) according to manufacture's  
167 manual. IL treated anammox granules (IM) were washed twice with double distilled water and  
168 freeze-dried before imaging.

169

170 **Anion exchange column**

171 IL-EPS was dissolved in 20 mM HEPES, pH 8.0 and passed through 0.2  $\mu$ m filter prior to being  
172 passed through purified anion exchange column connected to Amersham Akta fast protein  
173 liquid chromatography (FPLC). The IL-EPS mixture was loaded onto a Source15Q column pre-  
174 equilibrated with HEPES and eluted with a linear salt gradient of 95-275 mM NaCl. Fractions  
175 containing the targeted protein were combined and concentrated by centrifugation filter,  
176 molecular weight cut-off 3 kDa (Amicon®, Merck) to a concentration of 1 mg/mL as  
177 determined by Qubit Protein Assay Kit (Invitrogen™) and the Qubit 3.0 Fluorometer  
178 (Invitrogen™).

179

180 **SDS-PAGE of the soluble EPS**

181 20  $\mu$ L of the IL-EPS and fractions eluted from the anion exchange column by 245 and 280 mM  
182 NaCl (EPI F6, EPI F7) were denatured in Laemmli buffer (Bio-Rad) (1:1 (v/v)) for 10 min at  
183 98°C and were loaded onto pre-cast NuPAGE 4-12% (w/v) Bis-Tris 1.5-mm minigel  
184 (Invitrogen™). The electrophoresis was carried out at 180 V in NuPAGE MES SDS running  
185 buffer (50 mM Tris base, 50 mM MES, 0.1% (w/v) SDS, 1 mM EDTA. pH 7.3) for 40 min.  
186 After electrophoresis the gel was removed from the cassette, washed multiple times with double  
187 distilled water and stained with Coomassie Blue (1g Coomassie Brilliant Blue in methanol  
188 (50% (v/v)) and glacial acetic acid (10% v/v))) for 1 h. The gel was then destained with  
189 destaining solution (25% (v/v) methanol, 5% (v/v) acetic acid) until protein bands became  
190 visible. Glycoprotein was detected by periodic acid-Schiff (PAS) staining kit (Thermo Fischer  
191 Scientific Pierce Glycoprotein Staining Kit).

192

193 **LC-MS/MS analysis of gel bands**



194 200 and 170 kDa bands were excised from the SDS-PAGE gel and subjected to reduction,  
195 alkylation and in-gel tryptic digestion as described by Shevchenko et al.<sup>31</sup>. Following digestion,  
196 the peptides were eluted with 1:1 (v/v) water/acetonitrile (ACN) solution with 0.2% (v/v) TFA  
197 into a microtiter receiver plate by vacuum and then concentrated by vacuum centrifugation  
198 (miVac, SP Scientific).

199 Peptide analysis was performed by LCMS-TripleTOF 5600 (refer to Supporting Information  
200 for details). Peptides were identified using ProteinPilot 5.0 software Revision 4769 (AB  
201 SCIEX) with the Paragon database search algorithm (5.0.0.0.4767) and the integrated false  
202 discovery rate (FDR) analysis function. These protein data were searched against a protein  
203 reference database of translated predicted genes from metagenome assemblies constructed from  
204 previously sampled reactor gDNA. The metagenome contained a recovered complete genome  
205 of *Ca. Brocadia*<sup>32</sup> and also included five extant draft AnAOB genomes, enabling comparative  
206 analysis.

207

### 208 **Antibody generation**

209 Two rabbits were inoculated with polypeptide sequence cys-DIREITGVASDR, representing  
210 amino acid sequence 742-753 of BROSI\_A1236 and identified to be an exposed region of the  
211 protein<sup>33</sup>, in a three-month immunization protocol consisting of four injections on days 0, 30,  
212 50 and 80 (SABio, Singapore). The serum was collected and affinity purified from rabbit  
213 antiserum. Total IgG fractions (crude serum) of one rabbit were used as primary anti-  
214 BROSI\_A1236 antibody. Refer to Figure S1 for Dot Blot analysis of the rabbit sera binding to  
215 the BROSI\_A1236 polypeptide.

216

### 217 **Immunoblot analysis**

218 Proteins were transferred from the SDS-PAGE gel to a membrane using iBlot transfer system  
219 (Invitrogen™). The polyvinylidene difluoride (PVDF) membrane was blocked with PBS-T  
220 (137 mM NaCl, 12 mM PO<sub>4</sub><sup>3-</sup>, 2.7 mM KCl, 0.05% Tween®20, pH 7.4) and 5% (w/v) bovine  
221 serum albumin (BSA) for 1 h at 22°C. The primary antibody was then diluted 3000 times in  
222 blocking buffer and incubated for 2 h at 22°C. PVDF membrane was washed three times with  
223 PBS-T for 10 min before incubating with Goat anti-Rabbit IgG (H+L) Secondary Antibody,  
224 HRP (ThermoFisher Scientific) diluted 5000 times in blocking buffer for 1 h at 22°C in the  
225 dark. After incubation, the membrane was washed five times for 15 min with PBS-T. For  
226 immune detection, the blot was then developed in 1:1 (v/v) dilution of SuperSignal™ West  
227 Femto Trial Kit (ThermoFisher Scientific) to achieve the desired signal intensity in the  
228 Amersham Hypercassette™ Autoradiography Cassettes.

229 X-ray film (CARESTREAM Medical X-ray Green/MXG Film) was exposed to the blot in the  
230 cassette from 2 s to 10 min, depending on the intensity of the signal. The film was then inserted  
231 into an auto processor provided by Abnova for film development.

232

### 233 **Size exclusion chromatography (SEC) analysis with fluorescence detector**

234 SEC was performed using (i) a liquid chromatograph with pump (LC-20AD), (ii) a fluorescence  
235 detector (RF-20AXS), (iii) an auto sampler (SIL-20AHT), and (iv) a communication module  
236 (CMB-20A). The molecular weights (MW) of the EPS samples were estimated by passing 15  
237 µL of the filtered samples through an analytical scale SEC column (OHpak SB-804 HQ)  
238 following its guard column (OHpak SB-G). Tris buffer (25 mM Tris, pH 7.0 ± 0.1) was used  
239 as the mobile phase. The SEC column was calibrated using transferrin, serum albumin bovine,  
240 myoglobin and beta amylase obtained from Sigma Aldrich (the details are provided in  
241 Supporting Information (SI)).

242

243 **Global protein analysis of *Ca. B. sinica*-enriched granules**

244 Protein extraction was performed as previously described<sup>34</sup>. Briefly, lyophilized anammox  
245 granules were resuspended in extraction buffer and cells were lysed by bead beading. Cell  
246 debris was removed, and extracted proteins were precipitated overnight using trichloroacetic  
247 acid (TCA). Pellets were washed three times in 100% ice-cold acetone, dried, and resuspended  
248 in 100 mM HEPES (pH 7.5). Protein concentration for each sample was estimated in a single  
249 technical replicate using the Qubit Protein Assay Kit (Invitrogen) and the Qubit 3.0 Fluorometer  
250 (Invitrogen).

251 Protein samples were then subjected to preparative denaturing SDS-PAGE (refer to Supporting  
252 Information). Gels were Coomassie-stained (Bio-Safe Coomassie Stain, Bio-Rad) and the  
253 protein bands (1 x 1 x 0.08 cm) excised and subjected to reduction, alkylation and in-gel tryptic  
254 digestion, as described elsewhere<sup>31</sup>. Following digestion, peptides were recovered, dried and  
255 reconstituted in 5% formic acid prior to desalting and clean-up using StageTips<sup>35, 36</sup> prepared  
256 as previously described<sup>37</sup> with the modification that an additional layer of PorosOligo R2  
257 material (Applied Biosystems, Foster City, CA, USA) was added on top of the PorosOligo R3  
258 material. Following purification, peptides were eluted using 66% (v/v) ACN, dried using  
259 vacuum centrifugation and reconstituted in 0.1% (v/v) TFA/2% (v/v) ACN solution.

260 Peptides were subsequently analyzed by ultra-high-performance liquid chromatography  
261 (UHPLC) using an Easy-nLC1200 (Thermo Scientific) online system coupled to a Q Exactive  
262 High Field mass spectrometer (Thermo Scientific) (refer to Supporting Information for  
263 complete details). Raw data from the Q Exactive High Field were analyzed using MaxQuant v.  
264 1.6.3.4. Each experiment was defined as its own parameter group. The label-free quantification  
265 (LFQ) and the intensity based absolute quantification (iBAQ) features were enabled, and LFQ  
266 was separated in parameter groups. Oxidation of methionine was set as a variable modification,

267 and carbamidomethylation of cysteine was set as a fixed modification. The ‘match between  
268 runs’ feature was selected, while all other settings were left as default.

269 The raw data were searched against an inhouse-generated database containing the open reading  
270 frames from *Ca. Brocadia* bins recovered from metagenomics assembly of the *Ca. Brocadia*  
271 *sinica*-enriched reactor<sup>32</sup>.

272

### 273 **Carbohydrate analysis**

274 Carbohydrate analysis of *Ca. B. sinica* granules (GR) and the IL-EPS samples extracted from  
275 *Ca. B. sinica* granules, was performed by Shimadzu Gas Chromatography triple quadrupole  
276 mass spectrometer (GC-QqQ-MS/MS) in multiple reaction monitoring (MRM) mode. The  
277 samples were digested in 4 M TFA for 4 h at 100°C<sup>38</sup>.

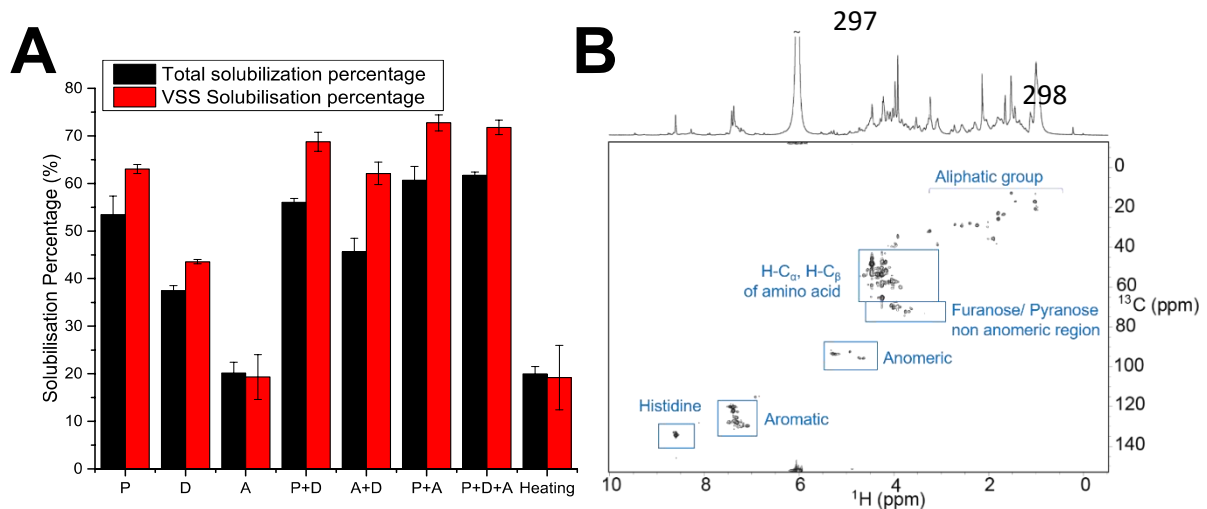
278

## 279 **Results**

### 280 **Profiling the contribution of EPS classes to anammox biofilm structure**

281 *Ca. B. sinica*-enriched granules (GR) (Figure S2) were digested with enzymes targeting general  
282 classes of extracellular polymers commonly found in environmental biofilms, including  
283 proteins (P), DNA (D) and  $\alpha$ - and  $\beta$ -glycans (A) (Figure 2A). Sludge from the laboratory-scale  
284 reactor enriched with *Ca. B. sinica* had a higher VSS content of 88% compared to industrial  
285 granules<sup>39</sup>. All enzymes achieved a higher degree of solubilization of the organic fraction  
286 relative to total biofilm, as indicated by low and high reductions in TSS and VSS respectively,  
287 following enzymatic digestions. This is likely due to the presence of inorganic minerals, which  
288 are common features of anammox biofilms (e.g. apatite)<sup>40</sup>. Digestion with pronase achieved a  
289 higher degree of solubilization than either DNase A,  $\alpha$  and  $\beta$  amylase or the control (i.e. heating  
290 only at 60 °C). A similar amount of VSS and TSS solubilization was observed in the control

291 sample as for  $\alpha$ - and  $\beta$ - amylase-treated granules (i.e. same buffers and heated to the same  
292 temperature). Thus, neither  $\alpha$ - or  $\beta$ -sugars contributes to the structure of the anammox EPS.  
293 Furthermore, high EPS solubilization is consistently achieved for granules treated with pronase,  
294 either by itself or coupled with DNase A,  $\alpha$ - or  $\beta$ -amylase. This suggests that proteins are  
295 important structural components of the *Ca. B. sinica*-enriched anammox EPS matrix.  
296



299  
300  
301 **Figure 2: (A) Percent solubilization of volatile and total solid in *Ca. B. sinica*-enriched granules (GR) grown**  
302 **in a laboratory reactor following digestion with enzymes: pronase E (P), DNase A (D),  $\alpha$  or  $\beta$  amylase (A).**  
303 **(B)  $^1\text{H}$ - $^{13}\text{C}$  HSQC and 1-D  $^1\text{H}$  NMR spectra of acid-digested anammox granules EPS (IL-EPS) in 4 M TFA-**  
304 **d (37.5 mg/mL) at 25°C showing a distribution of  $^1\text{H}$ - $^{13}\text{C}$  HSQC cross peaks that is consistent with the**  
305 **presence of protein and hexose-based sugars.**

306  
307 The heteronuclear single quantum coherence (HSQC) NMR spectrum of acid-digested  
308 anammox granule EPS (IL-EPS) (Figure 2B) shows that some polysaccharides were present  
309 along with proteins. This is illustrated by HSQC cross peaks at ( $\delta_{\text{H}}$ ,  $\delta_{\text{C}}$ ) of (4.8-5.3, 92.4-95.5),  
310 consistent with the anomeric region of polysaccharides<sup>41</sup> ( $\delta_{\text{H}}$  and  $\delta_{\text{C}}$  are the  $^1\text{H}$  and  $^{13}\text{C}$  chemical  
311 shifts in ppm respectively). It is therefore possible that polysaccharides not targeted by  $\alpha$ - or  $\beta$ -  
312 amylase co-exist with structural proteins (i.e. not  $\alpha$ - or  $\beta$ -glycans such as granulan or alginate-  
313 like exopolysaccharides)<sup>42</sup>. Another explanation could be that glycoproteins are a component

314 of the anammox biofilm EPS. Nonetheless, the spectrum is dominated by HSQC cross peaks at  
315 ( $\delta_H$ ,  $\delta_C$ ) of (4.2-4.8, 45.6-67.5), (7.2-7.6, 119.1-131.7) and (8.5-8.7, 130.7-136.7), which  
316 represent amino acid  $\alpha$ -regions and aromatics, and histidines, respectively, further supporting  
317 our finding that proteins dominate *Ca. B. sinica*-enriched granules<sup>43,44</sup>.

318

### 319 **Ionic liquid-based EPS extraction**

320 We therefore aimed to extract structural proteins from the *Ca. B. sinica*-enriched granules, and  
321 used ionic liquid 1-ethyl-3-methyl imidazolium acetate (EMIM-Ac) for this purpose given its  
322 demonstrated ability to dissolve recalcitrant polymers. The recovery yields of representative  
323 biofilm exopolymers (i.e. basic and acidic proteins, anionic, cationic and neutral  
324 polysaccharides) following dissolution in 40:60 (v/v) EMIM-Ac/DMAc with recovery by  
325 ethanol precipitation (i.e. anti-solvent), were determined (Figure S3). Recovery yields of  $54.1$   
326  $\pm 9.0$  and  $23.2 \pm 8.7\%$  (w/w) for basic and acidic proteins (i.e. cytochrome C and lipase)  
327 respectively were achieved following EMIM-Ac/DMAc solubilization and ethanol  
328 precipitation. EMIM-Ac/DMAc dissolution with ethanol precipitation is therefore a viable  
329 strategy for recovering extracellular proteins from anammox biofilms. Further, EMIM-  
330 Ac/DMAc coupled with ethanol as anti-solvent recovered neutral and cationic polysaccharides  
331 (i.e. cellulose and chitosan), consistent with what has been described in the literature<sup>45</sup>.

332 Anammox granules dissolved in EMIM-Ac/DMAc at 55°C (16 h) separated into two phases;  
333 an insoluble granular phase (IGS), and an ionic liquid soluble phase (IL-S) (Figure 1). The  
334 recovery yield following EMIM-Ac/DMAc solubilization and ethanol precipitation and dialysis  
335 was  $8.2 \pm 2.0\%$  (w/w). The recovered fraction subsequently separated during dialysis into a  
336 water soluble fraction (IL-EPS) and a water insoluble gel (IL-GEL).

337

338 **Ionic liquid treatment increases the permeability of, but does not fluidize, *Ca. B. sinica***  
339 **cells**

340 Ionic liquids are known to kill cells, which is believed to be due to osmotic shocking of cell  
341 membranes<sup>46</sup>. Live-dead stain of the anammox biofilms indicated both live and dead cells, even  
342 in the non-treated component (Figure 3A). Relative to the control, EMIM-Ac/DMAc treatment  
343 disrupted aggregate organization such that clusters of dead cells dominated and were less evenly  
344 distributed (Figure 3B). Nonetheless, there were also live and dead cells and the loss of order  
345 in how the cells are arranged could indicate that the EPS has been extracted.

346 *Planctomycetes* are Gram-negative bacteria with an outer membrane that contains eukaryotic-  
347 like phospholipids in the inner leaflet<sup>47</sup>. To investigate whether increased permeability was due  
348 to membrane fluidization, we used <sup>31</sup>P NMR to determine if anammox phospholipids are  
349 released into EMIM-Ac/DMAc upon dissolution. The phospholipid standard (i.e. asolectin  
350 from soybean) displayed a range of sharp spectral peaks at  $\delta_P$  -3 – 0 ppm, consistent with  
351 diesterified phosphates (Figure 3C, blue), demonstrating that phospholipids dissolved in  
352 EMIM-Ac/DMAc can be detected by <sup>31</sup>P NMR. In contrast, no <sup>31</sup>P NMR peaks were observed  
353 in the spectrum of EMIM-Ac/DMAc following anammox biofilm dissolution (IL-S) (Figure  
354 3C, green) apart from the reference phosphate peak (i.e. H<sub>3</sub>PO<sub>4</sub>) seen at  $\delta_P$  0 ppm. To support  
355 the hypothesis that cell lysis can be detected by <sup>31</sup>P NMR, the spectrum of planktonic  
356 *Pseudomonas aeruginosa* cells treated with lysozyme showed several sharp spectral peaks in  
357 the monoesterified and diesterified phosphate region (Figure 3C, red). The signal observed at  
358  $\delta_P$  0 ppm in every sample arose from the 7.5 mM H<sub>3</sub>PO<sub>4</sub> standard, where the neat H<sub>3</sub>PO<sub>4</sub> <sup>31</sup>P  
359 NMR spectra is shown in black.

360 It is possible that the constituents extracted by ionic liquid derived from inside the cells. While  
361 the red color of the gel phase following EMIM-Ac/DMAc treatment of the anammox biofilm

362 (Figure 1) could derive from intracellular Cyt-C heme proteins in anammox granules<sup>24</sup>, the <sup>31</sup>P

363 NMR spectrum nonetheless indicates that the cell membranes remain intact.

364



365

366

367

368

369

370

371

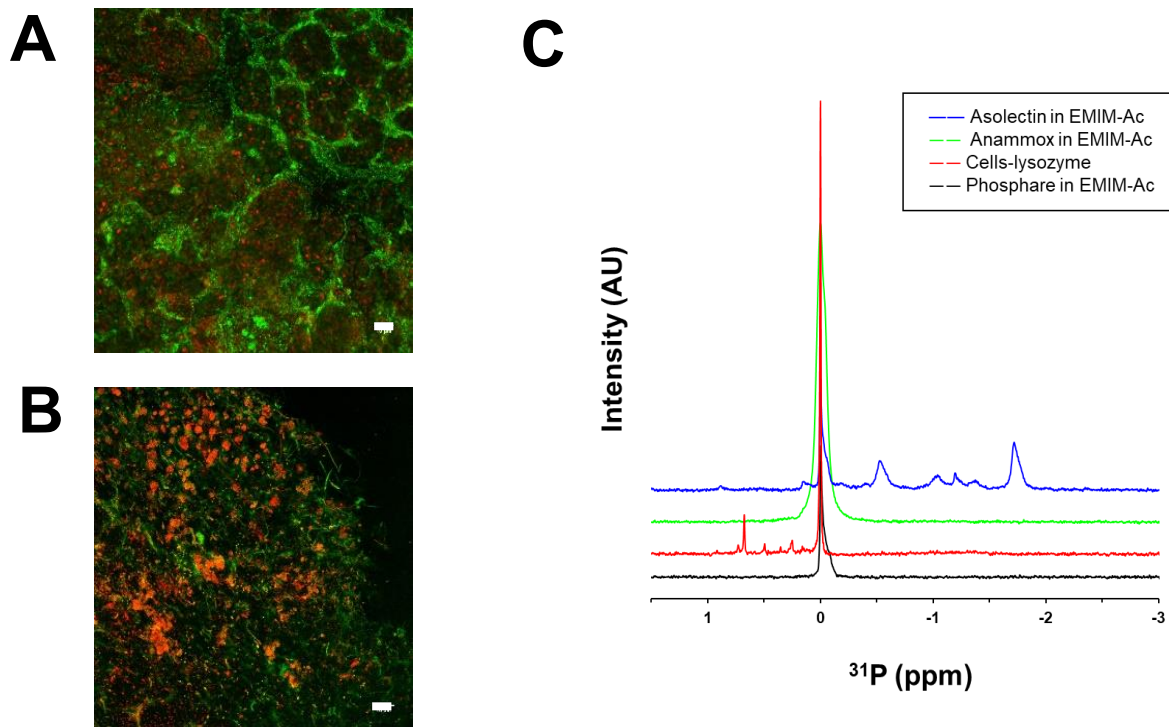
372

373

374

375

376



377 **Figure 3: Live (green)-dead (red) stain of *Ca. B. sinica* cells (GR) (A) without any treatment and (B)**

378 **following dissolution in 40:60 (v/v) EMIM-Ac/DMAc (IM) at 55°C for 6 h. Scale bar indicates 10 μm. (C)**

379 **<sup>31</sup>P NMR spectra of azolectin following dissolution in EMIM-Ac/DMAc (55°C, 6 h) (blue), *Ca. B. sinica*-**

380 **enriched granules following dissolution in EMIM-Ac/DMAc (IS) (55°C, 6 h) (green), lysozyme-treated**

381 ***Pseudomonas aeruginosa* planktonic cells (red) i.e. a positive control. 7.5 mM phosphoric acid was added to**

382 **all samples as a reference.**

383

### 384 **Isolation of extracellular protein**

385 The molecular weight (MW) distribution of anammox biofilm extracellular proteins, recovered

386 from EMIM-Ac/DMAc by ethanol precipitation, was described by SDS-PAGE with Coomassie

387 Blue, periodic acid-Schiff staining (Figure 4A). Major protein bands in the anammox biofilm

388 EPS extract (IL-EPS) (Figure 4A Lane 2) appear at 55, 60, 65, 170 and 200 kDa. A similar

389 protein MW profile was observed in the SDS-PAGE gel of the IL-GEL sample (Figure S4).

390 Thus the same high MW protein doublet dominates both the IL-EPS and IL-GEL, suggesting

391 that it can undergo a sol-gel transition. In subsequent processing of the IL-EPS by anion

392 exchange chromatography (AEC) the high MW doublet of proteins were concentrated in  
393 fractions eluted with 0.2M HEPES buffer with NaCl concentrate in the range of 245 and 280  
394 mM (i.e. 170 and 200 kDa, Figure 4A Lane 3). The AEC purified high MW proteins (EPI) also  
395 stained positive for periodic acid-Schiff (PAS) stain (Figure 4A Lane 4), indicating that the  
396 high MW protein doublet is glycosylated (i.e. glycoproteins)<sup>48</sup>. Gel permeation chromatography  
397 further confirmed the purity of the AEC purified protein where the sample was separated into  
398 two major peaks across the high MW range (… EPI F6, Figure 4B).

399

400

401

402

403

404

405

406

407

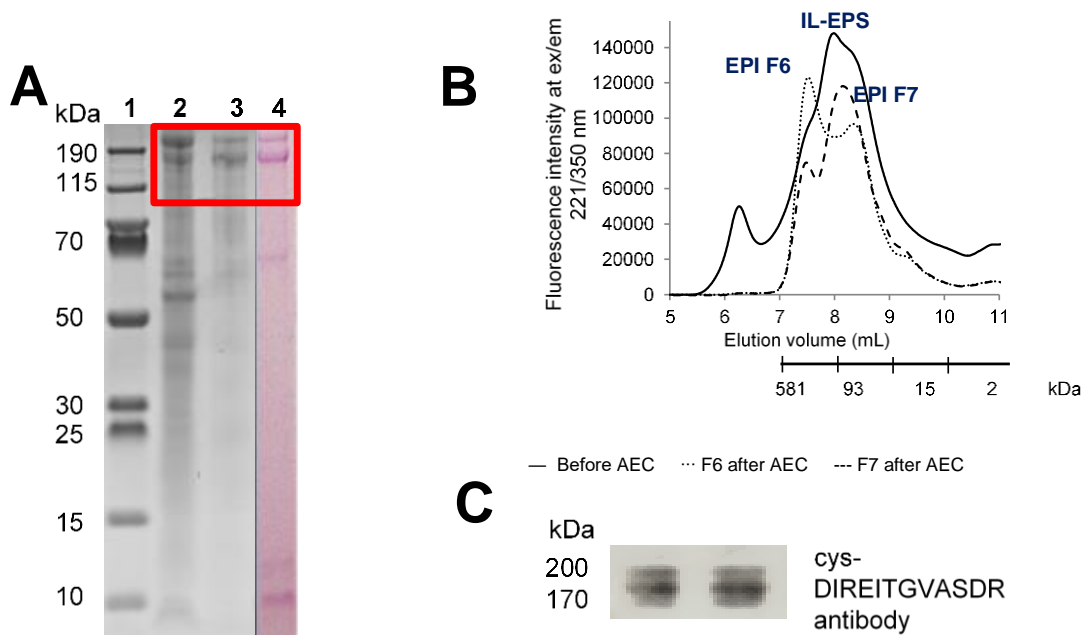
408

409

410

411

412 **Figure 4: (A) SDS-PAGE gel showing extracellular proteins extracted from *Ca. B. sinica*-enriched granules**  
413 **using EMIM-Ac/DMAc (IL-EPS, Lane 2), anion exchange chromatography (AEC)-purified anammox**  
414 **protein extract (EPI, Lane 3), and periodic acid-Schiff (PAS) stained SDS-PAGE gel showing positively**  
415 **stained high molecular weight glycoprotein doublet (Lane 4). Lane 1 is the PageRuler™ prestained protein**  
416 **ladder. (B) Size exclusion chromatogram profile of crude anammox EPS extract (IL-EPS) and anion**  
417 **exchange chromatography purified EPS fractions (EPI), showing effective AEC purification as well as**  
418 **simplification of chromatogram of sample F6 and F7 after AEC. (C) Immunoblotting validation by Western**  
419 **blot showing positive blot of BROSI\_A1236 doublet (EPI) to cys-DIREITGVASDR antibody.**

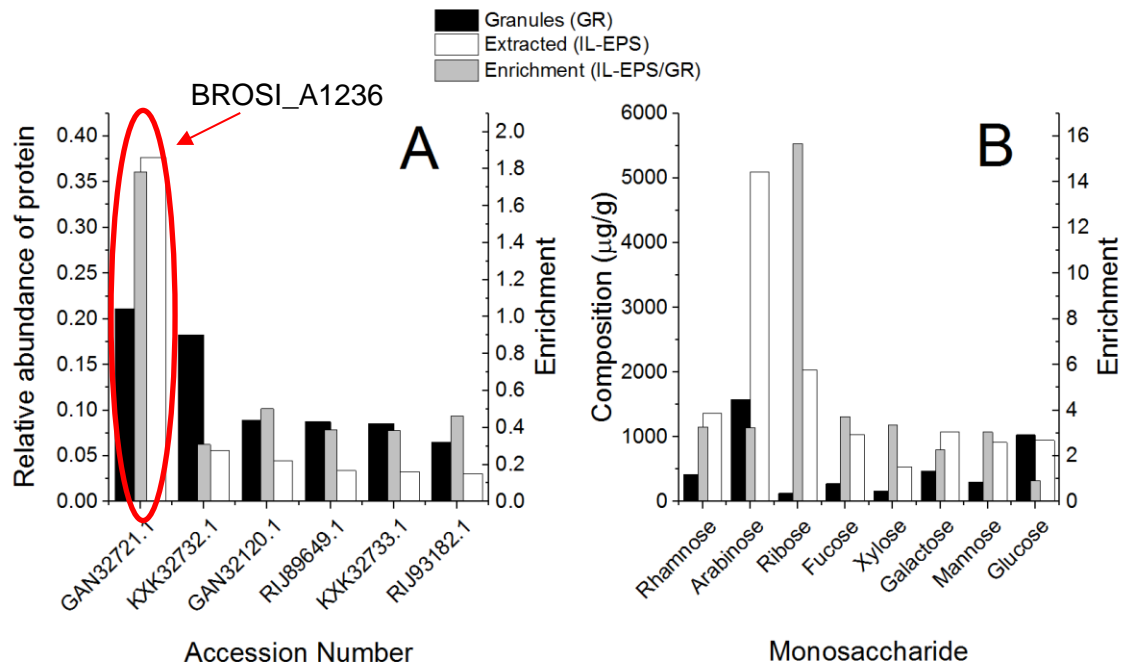


420

421 **Co-enrichment of surface layer (S-layer) glycoprotein with commonly o-glycosylating**  
422 **monosaccharides**

423 The AEC-purified proteins (EPI) extracted from *Ca. B. sinica*-enriched granules by EMIM-  
424 Ac/DMAc were analyzed by MS/MS and the identified polypeptide fragments mapped against  
425 a database for all bacteria. Two hypothetical proteins dominated, BROSI\_A1236 and  
426 UZ01\_01563, that were identical with the exception that BROSI\_A1236 has an additional 247  
427 amino acids at the N-terminus<sup>49</sup>. We henceforth refer to them as BROSI\_A1236. Immunoblot  
428 analysis of the isolated protein, using antibodies raised against amino acids 742-753 of  
429 BROSI\_A1236, further validated its identity as BROSI\_A1236 (Figure 4C; Figure 1). It is  
430 highly similar to putative S-layer protein KUSTD1514 (e-value: 0, protein 44%)<sup>50</sup>. The most  
431 highly similar abundant proteins in terms of iBAQ (i.e. > 5% abundance) in *Ca. B. sinica*-  
432 enriched granules (GR) and the EMIM-Ac extract (IL-EPS) are presented in Figure 5A, with  
433 the BROSI\_A1236 being the most abundant protein in the EPS prior to AEC purification (i.e.  
434 extracted directly by ionic liquid and recovered by ethanol, IL-EPS). There was a two-fold  
435 enrichment of BROSI\_A1236 following extraction by EMIM-Ac relative to the crude granules,  
436 to almost 40% abundance. It is likely, however, that the true abundance of BROSI\_A1236  
437 following EMIM-Ac/DMAc extraction was even higher given that mass spectrometry  
438 underestimates glycoprotein content due to inhibition of trypsin digestion by the sugars<sup>51</sup>.  
439 Hence, EMIM-Ac/DMAc extraction followed by ethanol recovery leads to a high enrichment  
440 of a putative S-layer glycoprotein from the extracellular matrix of the anammox granules.  
441 The anammox biofilm contains sugars, as demonstrated by the HSQC NMR spectrum of acid-  
442 digested IL extracted anammox EPS (IL-EPS) (Figure 2B). The concentrations of  
443 monosaccharides commonly associated with either exopolysaccharides or glycoproteins were  
444 measured, and the eight most abundant monosaccharides present in crude anammox biofilms  
445 (GR) and in the EMIM-Ac/DMAc soluble material (IL-EPS) are presented in Figure 5B. The

446 fraction of all sugars in the anammox biofilm was 0.45% (w/w), increasing to 1.3% (w/w) in  
447 the EMIM-Ac/DMAc extract (IL-EPS). Thus, sugars constitute only a small fraction of the dry  
448 weight of the *Ca. B. sinica*-enriched granule (GR), providing further evidence of the importance  
449 of proteins in the granule structure. An approximately three-fold increase was observed for all  
450 sugars except glucose and ribose, concomitant with a two-fold increase in glycoprotein  
451 BROSI\_A1236 (EPI). BROSI\_A1236 (EPI) is enriched in serine and threonine (11.8 and 16.0%  
452 respectively), which are the most commonly o-glycosylated<sup>52</sup> amino acids. Given that  
453 arabinose, xylose, fucose, rhamnose, mannose and galactose are co-enriched with  
454 BROSI\_A1236 (IL-EPS) in the extracted protein versus the crude anammox biofilm (GR), it is  
455 probable that they are appended to the putative S-layer glycoprotein BROSI\_A1236.  
456 Two protein bands and GPC peaks were observed from the SDS-PAGE gel and gel permeation  
457 chromatogram respectively of the AEC purified fractions (EPI F6 & F7). The high MW peak  
458 dominated in EPI F6 from AEC and the low MW peak dominated in EPI F7. These confirm the  
459 existence of two structurally similar glycoproteins (i.e. BROSI\_A1236 and UZ01\_01563), or  
460 reflect the different proteoforms of a single protein (e.g. in different glycosylation states).  
461



462

463

464 **Figure 5: (A) Relative abundance of dominant proteins (i.e. > 5% abundance (iBAQ)) in *Ca. B. sinica*-**  
 465 **enriched anammox granules (GR, black) and the water-soluble fraction extracted by EMIM-Ac/DMAc (IL-**  
 466 **EPS, white). Degree of enrichment of top six proteins before and after extraction from *Ca. B. sinica*-enriched**  
 467 **granules following dissolution in EMIM-Ac/DMAc (grey) (i.e. (iBAQ of water-soluble fraction (IL-EPS))/**  
 468 **(iBAQ of granules (GR))). (B) Dry weight composition of typical glycoprotein monosaccharides before and**  
 469 **after extraction from *Ca. B. sinica*-enriched granules by EMIM-Ac/DMAc (i.e. composition (µg/g) of water-**  
 470 **soluble fraction (IL-EPS)/ composition (µg/g) of granules (GR)). Degree of enrichment of monosaccharides**  
 471 **before and after extraction from *Ca. B. sinica*-enriched granules following dissolution in EMIM-Ac/DMAc**  
 472 **(grey).**

473

## 474 Discussion

475 We observed that proteins are key structural components of *Ca. B. sinica*-enriched biofilms and  
 476 demonstrated a means to extract and concentrate a putative S-layer glycoprotein using ionic  
 477 liquid 1-ethyl-3-methyl-imidazolium acetate (EMIM-Ac), which allowed for its subsequent  
 478 isolation and identification. It is very similar to putative surface layer proteins KUESTD1514

479 from *Ca. K. stuttgartiensis* anammox sludge and also to WP\_070066019.1 from *Ca. Brocadia*  
480 *sapporiensis* sludges<sup>53</sup>. Furthermore, while sugars were only minor components of the *Ca. B.*  
481 *sinica*-enriched biofilm, they were co-enriched along with the glycoprotein and thus likely exist  
482 in the biofilm predominately attached to proteins rather than as free polysaccharides.

483 While S-layers have been postulated to promote biofilm formation, as for *Tannerella forsythia*,  
484 the mechanism by which they achieve this is unknown. S-layers may appear as crystalline  
485 structures in the matrix as a result of cell-surface shedding<sup>26</sup>. However, it is not clear how  
486 crystalline structures might support biofilm formation. The means to extract and subsequently  
487 S-layer glycoproteins from biofilm matrices, as described here, will enable methods to be  
488 applied to describe the mechanism by which they contribute to the growth of other biofilms.  
489 Interestingly, part of the ethanol recovered IL-soluble fraction (IL-S) also formed a gel (IL-  
490 GEL) during dialysis. It is therefore possible that, in addition to performing role as a S-layer  
491 protein, Brosi\_A1236 could also contribute to biofilm formation by undergoing phase  
492 separation to a gel. One possible mechanism by which the putative S-layer protein contributes  
493 to anammox biofilm could therefore be that it mediates phase separation of the matrix into gels.  
494 This could further inform the role of S-layer protein in anammox biofilms, but possibly in  
495 biofilms more broadly.

496

497 To date, the only reported method of S-layer protein extraction from anammox biofilms was  
498 physical extraction by means of Potter homogenizer, which is known to disrupt cells<sup>25</sup>.  
499 Chaotropes such as lithium chloride (LiCl)<sup>54</sup> or guanidine hydrochloride (GnHCl)<sup>55</sup> are  
500 typically used in S-layer protein extractions. LiCl is believed to solubilize S-layer proteins in  
501 gram positive bacteria by disrupting the hydrogen bond between protein and secondary cell  
502 wall polysaccharides. Such treatments have not been demonstrated for biofilm and EPS  
503 solubilization and hence are not likely to be effective at facilitating the isolation of S-layer

504 proteins from extracellular matrices. Ionic liquids can isolate S-layer proteins from biofilm  
505 matrices because they are equally effective at solubilizing proteins as they are for recalcitrant  
506 polysaccharides like cellulose. Furthermore, they achieve this by disrupting intermolecular  
507 hydrogen bonds and increasing solvent order without destabilizing the solute or protein.  
508 Similar to LiCl and GnHCl, interactions between the cation and anion of ionic liquids (like  
509 EMIM-Ac) have chaotropic effects on the protein and kosmotropic effect on the solvent<sup>56</sup>. The  
510 exception to this is cytochrome c, where Fujita et al.<sup>57</sup> found that ionic liquid had a kosmotropic  
511 effect leading to its solubilization. Nonetheless, ionic liquids are good options for isolating  
512 extracellular proteins where it is important to preserve their tertiary structure, as would be  
513 required to describe the mechanism of the role of S-layer protein in biofilm formation, i.e. to  
514 describe their biophysical properties and roles in biofilms, higher order structures and how they  
515 interact with cells, other exopolymers and their environment. In addition, ionic liquid EPS  
516 extraction was also found here to cause minimal cell disruption as shown by the absence of the  
517 phosphate signal in the <sup>31</sup>P NMR analysis of the ionic liquid EPS extract supernatant (IL-S).

518  
519 Similarly, the means to solubilize EPS enables a range of approaches to be applied for assigning  
520 function, not least of all accurate quantification, but also immunofluorescence microscopy<sup>58</sup>,  
521 single molecular structural (e.g. circular dichroism)<sup>59</sup> and biophysical (e.g. optical tweezing)<sup>60</sup>  
522 analyses. Global quantitative profiling of anammox EPS components has also been applied  
523 widely to correlate EPS with certain process parameters, such as salinity resistance<sup>61</sup>, settling  
524 performance<sup>62</sup> and preservation techniques<sup>63</sup>. However, most studies assume that the key EPS  
525 are solubilized, which is challenging for the notoriously recalcitrant anammox EPS. Thus,  
526 isolating, non-destructively, extracellular polymers from the biofilm will lead to an improved  
527 understanding of their function in the anammox biofilm.

528

529 We illustrate with this study a non-destructive means to extract extracellular polymers from  
530 anammox granules. Additionally, this allows for the subsequent isolation of an S-layer  
531 glycoprotein, by anion exchange chromatography, which will enable more detailed structural  
532 and functional characterization of a putative S-layer protein from a complex, ecologically and  
533 industrially important biofilm.

534

## 535 **Acknowledgements**

536 This research was supported by the Singapore National Research Foundation under its  
537 Environment & Water Research Programme and administered by PUB, project number 1301-  
538 IRIS-59. SCELSE is funded by Singapore's Ministry of Education, National Research  
539 Federation, Nanyang Technological University (NTU), and National University of Singapore  
540 (NUS) and hosted by NTU in partnership with NUS. The authors are thankful to Dr Sharon  
541 Longford for proofreading the paper, Dr Henrik Kjeldal and Dr Mads Toft Søndergaard for  
542 global protein analysis and Mr Lim Teck Kwang for LC-MS/MS analysis of gel bands.

543

## 544 **References**

- 545 1. Hannides, C. C. S., Migrant solution to the anammox mystery. *Proceedings of the*  
546 *National Academy of Sciences* **2014**, *111*, (44), 15604-15605.
- 547 2. Hu, Z.; Lotti, T.; de Kreuk, M.; Kleerebezem, R.; van Loosdrecht, M.; Kruit, J.; Jetten,  
548 M. S. M.; Kartal, B., Nitrogen removal by a nitrification-anammox bioreactor at low  
549 temperature. *Applied and Environmental Microbiology* **2013**, *79*, (8), 2807-2812.
- 550 3. Ali, M.; Okabe, S., Anammox-based technologies for nitrogen removal: Advances in  
551 process start-up and remaining issues. *Chemosphere* **2015**, *141*, 144-153.
- 552 4. Zhang, L.; Narita, Y.; Gao, L.; Ali, M.; Oshiki, M.; Ishii, S.; Okabe, S., Microbial  
553 competition among anammox bacteria in nitrite-limited bioreactors. *Water Research* **2017**,  
554 *125*, 249-258.
- 555 5. Innerebner, G.; Insam, H.; Franke-Whittle, I. H.; Wett, B., Identification of anammox  
556 bacteria in a full-scale deammonification plant making use of anaerobic ammonia oxidation.  
557 *Systematic and Applied Microbiology* **2007**, *30*, (5), 408-412.



- 558 6. Suarez, C.; Hermansson, M.; Persson, F., Predation of nitrification–anammox biofilms  
559 used for nitrogen removal from wastewater. *FEMS Microbiology Ecology* **2015**, *91*, (11).
- 560 7. Ding, Z.; Bourven, I.; Guibaud, G.; van Hullebusch, E. D.; Panico, A.; Pirozzi, F.;  
561 Esposito, G., Role of extracellular polymeric substances (EPS) production in bioaggregation:  
562 application to wastewater treatment. *Applied Microbiology and Biotechnology* **2015**, *99*, (23),  
563 9883-9905.
- 564 8. Seviour, T.; Derlon, N.; Dueholm, M. S.; Flemming, H.-C.; Girbal-Neuhauser, E.;  
565 Horn, H.; Kjelleberg, S.; van Loosdrecht, M. C. M.; Lotti, T.; Malpei, M. F.; Nerenberg, R.;  
566 Neu, T. R.; Paul, E.; Yu, H.; Lin, Y., Extracellular polymeric substances of biofilms:  
567 Suffering from an identity crisis. *Water Research* **2019**, *151*, 1-7.
- 568 9. Feng, C.; Lotti, T.; Lin, Y.; Malpei, F., Extracellular polymeric substances extraction  
569 and recovery from anammox granules: Evaluation of methods and protocol development.  
570 *Chemical Engineering Journal* **2019**, *374*, 112-122.
- 571 10. Fernandez, I.; Bravo, J.; Mosquera-Corral, A.; Pereira, A.; Campos, J.; Mendez, R.;  
572 Melo, L., Influence of the shear stress and salinity on Anammox biofilms formation:  
573 modelling results. *Bioprocess and Biosystems Engineering* **2014**, *37*, (10), 1955-1961.
- 574 11. Ma, C.; Jin, R.-C.; Yang, G.-F.; Yu, J.-J.; Xing, B.-S.; Zhang, Q.-Q., Impacts of  
575 transient salinity shock loads on Anammox process performance. *Bioresource Technology*  
576 **2012**, *112*, 124-130.
- 577 12. Windey, K.; De Bo, I.; Verstraete, W., Oxygen-limited autotrophic nitrification–  
578 denitrification (OLAND) in a rotating biological contactor treating high-salinity wastewater.  
579 *Water Research* **2005**, *39*, (18), 4512-4520.
- 580 13. Hou, X.; Liu, S.; Zhang, Z., Role of extracellular polymeric substance in determining  
581 the high aggregation ability of anammox sludge. *Water Research* **2015**, *75*, 51-62.
- 582 14. Jia, F.; Yang, Q.; Liu, X.; Li, X.; Li, B.; Zhang, L.; Peng, Y., Stratification of  
583 extracellular polymeric substances (EPS) for aggregated anammox microorganisms.  
584 *Environmental Science & Technology* **2017**, *51*, (6), 3260-3268.
- 585 15. Gonzalez-Gil, G.; Sougrat, R.; Behzad, A. R.; Lens, P. N.; Saikaly, P. E., Microbial  
586 community composition and ultrastructure of granules from a full-scale anammox reactor.  
587 *Microbial Ecology* **2015**, *70*, (1), 118-131.
- 588 16. Ni, B.-J.; Hu, B.-L.; Fang, F.; Xie, W.-M.; Kartal, B.; Liu, X.-W.; Sheng, G.-P.;  
589 Jetten, M.; Zheng, P.; Yu, H.-Q., Microbial and physicochemical characteristics of compact  
590 anaerobic ammonium-oxidizing granules in an upflow anaerobic sludge blanket reactor.  
591 *Applied and Environmental Microbiology* **2010**, *76*, (8), 2652-2656.
- 592 17. Ni, S.-Q.; Sun, N.; Yang, H.; Zhang, J.; Ngo, H. H., Distribution of extracellular  
593 polymeric substances in anammox granules and their important roles during anammox  
594 granulation. *Biochemical Engineering Journal* **2015**, *101*, 126-133.
- 595 18. Vázquez-Padín, J.; Mosquera-Corral, A.; Campos, J. L.; Méndez, R.; Revsbech, N. P.,  
596 Microbial community distribution and activity dynamics of granular biomass in a CANON  
597 reactor. *Water Research* **2010**, *44*, (15), 4359-4370.

- 598 19. Vlaeminck, S. E.; Terada, A.; Smets, B. F.; De Clippeleir, H.; Schaubroeck, T.; Bolca,  
599 S.; Demeestere, L.; Mast, J.; Boon, N.; Carballa, M.; Verstraete, W., Aggregate size and  
600 architecture determine microbial activity balance for one-stage partial nitrification and  
601 anammox. *Applied and Environmental Microbiology* **2010**, *76*, (3), 900-909.
- 602 20. Volcke, E. I. P.; Picioreanu, C.; De Baets, B.; van Loosdrecht, M. C. M., Effect of  
603 granule size on autotrophic nitrogen removal in a granular sludge reactor. *Environmental*  
604 *Technology* **2010**, *31*, (11), 1271-1280.
- 605 21. Zhang, Z.; Gong, Z.; Liu, S.; Ni, J., Extracellular polymeric substances extraction  
606 induced the increased purification performance of percoll density gradient centrifugation for  
607 anammox bacteria. *Chemical Engineering Journal* **2016**, *287*, 529-536.
- 608 22. Almstrand, R.; Persson, F.; Daims, H.; Ekenberg, M.; Christensson, M.; Wilén, B.-M.;  
609 Sörensson, F.; Hermansson, M., Three-dimensional stratification of bacterial biofilm  
610 populations in a moving bed biofilm reactor for nitrification-anammox. *International journal of*  
611 *molecular sciences* **2014**, *15*, (2), 2191-2206.
- 612 23. Liu, X.-M.; Sheng, G.-P.; Luo, H.-W.; Zhang, F.; Yuan, S.-J.; Xu, J.; Zeng, R. J.; Wu,  
613 J.-G.; Yu, H.-Q., Contribution of Extracellular Polymeric Substances (EPS) to the Sludge  
614 Aggregation. *Environmental Science & Technology* **2010**, *44*, (11), 4355-4360.
- 615 24. Kartal, B.; Keltjens, J. T., Anammox Biochemistry: a Tale of Heme *c* Proteins. *Trends*  
616 *in Biochemical Sciences* **2016**, *41*, (12), 998-1011.
- 617 25. van Teeseling, M. C. F.; de Almeida, N. M.; Klingl, A.; Speth, D. R.; Op den Camp,  
618 H. J. M.; Rachel, R.; Jetten, M. S. M.; van Niftrik, L., A new addition to the cell plan of  
619 anammox bacteria: "*Candidatus* Kuenenia stuttgartiensis" has a protein surface layer as the  
620 outermost layer of the cell. *Journal of bacteriology* **2014**, *196*, (1), 80-89.
- 621 26. Boleij, M.; Pabst, M.; Neu, T. R.; van Loosdrecht, M. C. M.; Lin, Y., Identification of  
622 glycoproteins isolated from extracellular polymeric substances of full-scale anammox  
623 granular sludge. *Environmental Science & Technology* **2018**, *52*, (22), 13127-13135.
- 624 27. Posch, G.; Pabst, M.; Brecker, L.; Altmann, F.; Messner, P.; Schäffer, C.,  
625 Characterization and scope of S-layer protein O-glycosylation in *Tannerella forsythia*. *The*  
626 *Journal of biological chemistry* **2011**, *286*, (44), 38714-38724.
- 627 28. Duan, Y.; Freyburger, A.; Kunz, W.; Zollfrank, C., Cellulose and chitin composite  
628 materials from an ionic liquid and a green co-solvent. *Carbohydrate Polymers* **2018**, *192*,  
629 159-165.
- 630 29. Rice, E. W.; Bridgewater, L.; American Public Health, A.; American Water Works,  
631 A.; Water Environment, F., *Standard methods for the examination of water and wastewater*.  
632 American Public Health Association: Washington, D.C., 2012.
- 633 30. Seviour, T.; Weerachanchai, P.; Hinks, J.; Roizman, D.; Rice, S. A.; Bai, L.; Lee, J.-  
634 M.; Kjelleberg, S., Solvent optimization for bacterial extracellular matrices: a solution for the  
635 insoluble. *RSC Advances* **2015**, *5*, (10), 7469-7478.

- 636 31. Shevchenko, A.; Tomas, H.; Havli, J.; Olsen, J. V.; Mann, M., In-gel digestion for  
637 mass spectrometric characterization of proteins and proteomes. *Nature Protocols* **2007**, *1*,  
638 2856.
- 639 32. Liu, X.; Arumugam, K.; Natarajan, G.; Seviour, T. W.; Drautz-Moses, D. I.; Wuertz,  
640 S.; Law, Y.; Williams, R. B. H., Draft Genome Sequence of a “*Candidatus Brocadia*”  
641 Bacterium Enriched from Activated Sludge Collected in a Tropical Climate. *Genome*  
642 *Announcements* **2018**, *6*, (19), e00406-18.
- 643 33. Schafferhans, A.; Kajan, L.; Richter, L.; Roos, M.; Bernhofer, M.; Hamp, T.;  
644 Yachdav, G.; Rost, B.; Hecht, M.; Goldberg, T.; Kloppmann, E.; Schneider, R.; Vriend, G.;  
645 Sander, C.; Ben-Tal, N.; Bromberg, Y.; Hönigschmid, P.; Ashkenazy, H.; Punta, M.;  
646 Schlessinger, A., PredictProtein—an open resource for online prediction of protein structural  
647 and functional features. *Nucleic Acids Research* **2014**, *42*, (W1), W337-W343.
- 648 34. Hansen, S. H.; Stensballe, A.; Nielsen, P. H.; Herbst, F.-A., Metaproteomics:  
649 Evaluation of protein extraction from activated sludge. *PROTEOMICS* **2014**, *14*, (21-22),  
650 2535-2539.
- 651 35. Rappsilber, J.; Mann, M.; Ishihama, Y., Protocol for micro-purification, enrichment,  
652 pre-fractionation and storage of peptides for proteomics using StageTips. *Nature Protocols*  
653 **2007**, *2*, 1896.
- 654 36. Rappsilber, J.; Ishihama, Y.; Mann, M., Stop and Go Extraction Tips for Matrix-  
655 Assisted Laser Desorption/Ionization, Nanoelectrospray, and LC/MS Sample Pretreatment in  
656 Proteomics. *Analytical Chemistry* **2003**, *75*, (3), 663-670.
- 657 37. Danielsen, H. N.; Hansen, S. H.; Herbst, F.-A.; Kjeldal, H.; Stensballe, A.; Nielsen, P.  
658 H.; Dueholm, M. S., Direct Identification of Functional Amyloid Proteins by Label-Free  
659 Quantitative Mass Spectrometry. *Biomolecules* **2017**, *7*, (3), 58.
- 660 38. Dallies, N.; François, J.; Paquet, V., A new method for quantitative determination of  
661 polysaccharides in the yeast cell wall. Application to the cell wall defective mutants of  
662 *Saccharomyces cerevisiae*. *Yeast* **1998**, *14*, (14), 1297-1306.
- 663 39. Lin, Y. M.; Lotti, T.; Sharma, P. K.; van Loosdrecht, M. C. M., Apatite accumulation  
664 enhances the mechanical property of anammox granules. *Water Research* **2013**, *47*, (13),  
665 4556-4566.
- 666 40. Johansson, S.; Rusalleda, M.; Colprim, J., Phosphorus recovery through biologically  
667 induced precipitation by partial nitritation-anammox granular biomass. *Chemical Engineering*  
668 *Journal* **2017**, *327*, 881-888.
- 669 41. Seviour, T.; Lambert, L. K.; Pijuan, M.; Yuan, Z., Structural Determination of a Key  
670 Exopolysaccharide in Mixed Culture Aerobic Sludge Granules Using NMR Spectroscopy.  
671 *Environmental Science & Technology* **2010**, *44*, (23), 8964-8970.
- 672 42. Seviour, T.; Yuan, Z.; van Loosdrecht, M. C. M.; Lin, Y., Aerobic sludge granulation:  
673 A tale of two polysaccharides? *Water Research* **2012**, *46*, (15), 4803-4813.

- 674 43. Messner, P.; Wugeditsch, T.; Gooley, A. A.; Zachara, N. E.; Puchberger, M.; Kosma,  
675 P., Structural heterogeneity in the core oligosaccharide of the S-layer glycoprotein from  
676 *Aneurinibacillus thermoaerophilus* DSM 10155. *Glycobiology* **1999**, *9*, (8), 787-795.
- 677 44. Diehl, B. G.; Watts, H. D.; Kubicki, J. D.; Regner, M. R.; Ralph, J.; Brown, N. R.,  
678 Towards lignin-protein crosslinking: amino acid adducts of a lignin model quinone methide.  
679 *Cellulose* **2014**, *21*, (3), 1395-1407.
- 680 45. Liebert, T.; Heinze, T., Interaction of ionic liquids with polysaccharides. 5. Solvents  
681 and reaction media for the modification of cellulose. *BioResources* **2008**, *3*, (2).
- 682 46. Hodyna, D.; Kovalishyn, V.; Semenyuta, I.; Blagodatnyi, V.; Rogalsky, S.;  
683 Metelytsia, L., Imidazolium ionic liquids as effective antiseptics and disinfectants against  
684 drug resistant *S. aureus*: In silico and in vitro studies. *Computational Biology and Chemistry*  
685 **2018**, *73*, 127-138.
- 686 47. Devos, D. P., PVC bacteria: variation of, but not exception to, the Gram-negative cell  
687 plan. *Trends in Microbiology* **2014**, *22*, (1), 14-20.
- 688 48. Wan, L.; van Huystee, R. B., Rapid determination of glycoproteins and glycopeptides  
689 by periodic acid Schiff reagent dot-blotting assay on nitrocellulose membrane. *Journal of*  
690 *Agricultural and Food Chemistry* **1993**, *41*, (6), 896-898.
- 691 49. Bethesda (MD): National Library of Medicine (US), N. C. f. B. I. Protein [Internet].  
692 <https://www.ncbi.nlm.nih.gov/protein/762180679> (6 July 2019),
- 693 50. Perras, A. K.; Daum, B.; Ziegler, C.; Takahashi, L. K.; Ahmed, M.; Wanner, G.;  
694 Klingl, A.; Leitinger, G.; Kolb-Lenz, D.; Gribaldo, S.; Auerbach, A.; Mora, M.; Probst, A. J.;  
695 Bellack, A.; Moissl-Eichinger, C., S-layers at second glance? Altiarchaeal grappling hooks  
696 (hami) resemble archaeal S-layer proteins in structure and sequence. *Frontiers in*  
697 *Microbiology* **2015**, *6*, (543).
- 698 51. Bailey, U.-M.; Schulz, B. L., Deglycosylation systematically improves N-glycoprotein  
699 identification in liquid chromatography–tandem mass spectrometry proteomics for analysis of  
700 cell wall stress responses in *Saccharomyces cerevisiae* lacking Alg3p. *Journal of*  
701 *Chromatography B* **2013**, *923-924*, 16-21.
- 702 52. O'Connell, B. C.; Tabak, L. A., A Comparison of Serine and Threonine O-  
703 Glycosylation by UDP-GaINAc:Polypeptide N-Acetylgalactosaminyltransferase. *Journal of*  
704 *Dental Research* **1993**, *72*, (12), 1554-1558.
- 705 53. Schuster, B.; Sleytr, U. B., Relevance of glycosylation of S-layer proteins for cell  
706 surface properties. *Acta biomaterialia* **2015**, *19*, 149-157.
- 707 54. Johnson, B.; Selle, K.; O'Flaherty, S.; Goh, Y. J.; Klaenhammer, T., Identification of  
708 extracellular surface-layer associated proteins in *Lactobacillus acidophilus* NCFM.  
709 *Microbiology (Reading, England)* **2013**, *159*, (Pt 11), 2269-2282.
- 710 55. Austin, J. W.; Stewart, M.; Murray, R. G., Structural and chemical characterization of  
711 the S layer of a *Pseudomonas*-like bacterium. *Journal of bacteriology* **1990**, *172*, (2), 808-  
712 817.

- 713 56. Zhao, H., Are ionic liquids kosmotropic or chaotropic? An evaluation of available  
714 thermodynamic parameters for quantifying the ion kosmotropicity of ionic liquids. *Journal of*  
715 *Chemical Technology & Biotechnology* **2006**, *81*, (6), 877-891.
- 716 57. Fujita, K.; MacFarlane, D. R.; Forsyth, M.; Yoshizawa-Fujita, M.; Murata, K.;  
717 Nakamura, N.; Ohno, H., Solubility and Stability of Cytochrome *c* in Hydrated Ionic Liquids:  
718 Effect of Oxo Acid Residues and Kosmotropicity. *Biomacromolecules* **2007**, *8*, (7), 2080-  
719 2086.
- 720 58. Karnati, S.; Oruqaj, G.; Janga, H.; Tumpara, S.; Colasante, C.; Van Veldhoven, P.;  
721 Braverman, N.; Pilatz, A.; J. Mariani, T.; Baumgart-Vogt, E., *PPAR $\alpha$ -mediated peroxisome*  
722 *induction compensates PPAR $\gamma$ -deficiency in bronchiolar club cells*. 2018; Vol. 13, p  
723 e0203466.
- 724 59. Greenfield, N. J., Using circular dichroism spectra to estimate protein secondary  
725 structure. *Nature protocols* **2006**, *1*, (6), 2876-2890.
- 726 60. Dong, J.; Castro, C.; Cunningham Boyce, M.; J Lang, M.; Lindquist, S., *Optical*  
727 *Trapping with High Forces Reveals Unexpected Behaviors of Prion Fibrils*. 2010; Vol. 17, p  
728 1422-30.
- 729 61. Xing, B.-S.; Guo, Q.; Yang, G.-F.; Zhang, Z.-Z.; Li, P.; Guo, L.-X.; Jin, R.-C., The  
730 properties of anaerobic ammonium oxidation (anammox) granules: Roles of ambient  
731 temperature, salinity and calcium concentration. *Separation and Purification Technology*  
732 **2015**, *147*, 311-318.
- 733 62. Chen, H.; Hu, H.-Y.; Chen, Q.-Q.; Shi, M.-L.; Jin, R.-C., Successful start-up of the  
734 anammox process: Influence of the seeding strategy on performance and granule properties.  
735 *Bioresource Technology* **2016**, *211*, 594-602.
- 736 63. Xing, B.-S.; Guo, Q.; Jiang, X.-Y.; Chen, Q.-Q.; Li, P.; Ni, W.-M.; Jin, R.-C.,  
737 Influence of preservation temperature on the characteristics of anaerobic ammonium  
738 oxidation (anammox) granular sludge. *Applied Microbiology and Biotechnology* **2016**, *100*,  
739 (10), 4637-4649.
- 740
- 741